HHS Public Access

Author manuscript

Otol Neurotol. Author manuscript; available in PMC 2020 July 01.

Published in final edited form as:

Otol Neurotol. 2019 July ; 40(6): 736–744. doi:10.1097/MAO.0000000000002164.

Intracochlear Pressure Transients During Cochlear Implant Electrode Insertion: Effect of Micro-mechanical Control on Limiting Pressure Trauma

Renee M. Banakis Hartl[1], **Christopher Kaufmann**[2], **Marlan R. Hansen**[2], and **Daniel J. Tollin**[1,3]

[1]Department of Otolaryngology, University of Colorado School of Medicine, Aurora, CO

[2]Department of Otolaryngology - Head & Neck Surgery, University of Iowa Hospitals and Clinics, Iowa City, IA

[3]Department of Physiology and Biophysics, University of Colorado School of Medicine, Aurora, CO

Abstract

Hypothesis: Use of micro-mechanical control during cochlear implant (CI) electrode insertion will result in reduced number and magnitude of pressure transients when compared with standard insertion by hand.

Introduction: With increasing focus on hearing preservation during CI surgery, atraumatic electrode insertion is of the utmost importance. It has been established that large intracochlear pressure spikes can be generated during the insertion of implant electrodes. Here, we examine the effect of utilizing a micro-mechanical insertion control tool on pressure trauma exposures during implantation.

Methods: Human cadaveric heads were surgically prepared with an extended facial recess. Electrodes from three manufacturers were placed both by utilizing a micro-mechanical control tool and by hand. Insertions were performed at three different rates: 0.2 mm/s, 1.2 mm/s, and 2 mm/s (n=20 each). Fiber-optic sensors measured pressures in scala vestibuli and tympani.

Results: Electrode insertion produced pressure transients up to 174 dB SPL. ANOVA revealed that pressures were significantly lower when utilizing the micro-mechanical control device compared with insertion by hand ($p<<0.001$). No difference was noted across electrode type or speed. Chi-square analysis showed a significantly lower proportion of insertions contained pressure spikes when the control system was used ($p<<0.001$).

Conclusion: Results confirm previous data that suggest CI electrode insertion can cause pressure transients with intensities similar to those elicited by high-level sounds. Results suggest that the use of a micro-mechanical insertion control system may mitigate trauma from pressure events,

Correspondence: Renee M Banakis Hartl, MD, AuD, University of Colorado School of Medicine, Department of Otolaryngology, 12631 E. 17th Ave, MS B205, Aurora, CO 80045, United States, Tele: 303-724-1957, Fax: 303-724-1961, address: Renee.BanakisHartl@ucdenver.edu.

Conflict of Interest Statement: CK and MRH are co-founders of iotaMotion, Inc.

both by reducing the amplitude and the number of pressure spikes resulting from CI electrode insertion.

Keywords

cochlear implant; insertion trauma; intracochlear pressure; micro-mechanical control; automated insertion; insertion tool

Introduction:

Since the introduction of cochlear implants (CIs) for the treatment of sensorineural hearing loss, increasing amounts of evidence have demonstrated improved performance outcomes for patients with greater amounts of preserved residual hearing[1–6]. Focus on preserving residual hearing during implantation surgery has become of the utmost importance, with emphasis on optimizing both electrode design[7,8] and surgical techniques[7,9–12] as means toward minimizing insertion-related trauma that could cause post-implantation loss of residual hearing. Further, intracochlear trauma is associated with poorer CI performance even in ears with profound preoperative hearing loss[13].

While the exact mechanisms of postoperative loss of residual hearing remain elusive, several recent investigations have confirmed the presence of potentially damaging insertion-related trauma in measurement of intracochlear fluid pressures[14–18]. Large transient pressure spikes during CI insertions have been recorded, which may reflect large fluid shifts related to the presence of the electrode or mechanical trauma from contact with the delicate structures of the sensory epithelium. Regardless of mechanism, it is possible that one manner of mitigating postoperative loss of residual hearing is the utilization of surgical techniques associated with less pressure-related trauma.

One surgical technique that has been proposed is the development of micromechanical insertion devices which could theoretically reduce insertion-related cochlear trauma by improving precision and by limiting human variability and error. To this end we have developed a robotic-assisted CI insertion system aimed at reducing electrode insertion trauma and enabling post-surgical, remote electrode position adjustments[19,20]. Other CI robotic systems include fully-automated insertion systems[21–27] with features such as patient-specific planning based on individual temporal bone and cochlear geometry determined from preoperative imaging[27]. These robotic systems are capable of controlling electrode insertion rates, angle, and distance for increased overall precision, but their larger size and complex setup may limit surgeon visibility and intraoperative flexibility, potentially limiting their clinical utility.

Several preliminary investigations have demonstrated reduced insertion forces with early prototypes of these types of tools[21,24,28]; however, measurement of force is an indirect way of estimating cochlear input and insertion-related trauma. Here, we aim to fill this knowledge gap and directly characterize cochlear input by measuring intracochlear pressures during electrode insertions. Differences in pressure levels between traditional electrode insertions by hand and with the use of a robotics-assisted micro-mechanical control device

were characterized with the aim of more accurate assessment of the relative trauma risk from each technique.

Methods:

We collected and analyzed data from four ears in fresh-frozen whole cadaveric heads with intact temporal bones (MD Global, Aurora, CO, USA). The use of cadaveric human tissue was in compliance with the University of Colorado Anschutz Medical Campus Institutional Biosafety Committee and Review Board (COMIRB EXEMPT #14-1464).

Temporal Bone Preparation:

Temporal bone specimens were prepared as previously described[14,15,29–33]. Intact, whole cadaveric heads were inspected to rule out injury or disease after thawing overnight in warm water. Specimens were each surgically prepared with a canal-wall-up mastoidectomy with an extended facial recess approach, and the cochlear promontory was blue-lined near the oval and round windows in preparation for pressure probe placement. Specimens were suspended with a Mayfield Clamp (Integra Lifesciences Corp., Plainsboro, NJ, U.S.A.) attached to a stainless-steel baseplate. A fine pick was used to create cochleostomies into the scala tympani (ST) and scala vestibuli (SV) under water to prevent air entry into the cochlea. Fiber-optic pressure sensors (FOP-M260-ENCAP, FISO Inc., Quebec, QC, Canada) were inserted (Figure 1A) into the scalae and sealed in place with alginate dental impression material (Jeltrate; Dentsply International Inc., York, PA).

Sound Presentation, Data Acquisition, and Baseline Acoustic Measurements:

Baseline acoustic measurements for each specimen are required in order to generate the transfer functions used to calculate estimated equivalent ear canal pressures for each insertion. Acoustic stimuli were presented as described previously[14,15,29–33] in a double-walled, sound-attenuating chamber (IAC Inc., Bronx, NY). Digitally generated stimuli were presented via a closed-field magnetic speaker (MF1; Tucker-Davis Technologies Inc., Alachua, FL) coupled directly to the ear with a foam insert. An external sound card (Hammerfall Multiface II, RME, Haimhausen, Germany) amplified with one channel of a stereo amplifier (TDT SA1) drove the speaker. Sound intensity in the ear canal was measured with a probe-tube microphone (type 4182; Bruel & Kjaer, Naerum, Denmark). Acoustic stimuli for calculation of transfer functions consisted of short (1s duration) tone pips between 100 and 12000 Hz ramped on and off with one half (5 ms) of a Hanning window.

The fiber-optic sensors were factory-calibrated and sensitivity was verified by normalizing the sensor response to laser Doppler vibrometer (LDV) displacement measurements made while generating a known motion in a cup of fluid controlled by a B&K mini-shaker (Bruel & Kjaer Type 4810, Naerum, Denmark). Out-of-plane velocities were measured with a single-axis LDV (OFV-534 & OFV-5000; Polytec Inc., Irvine, CA) mounted to a dissecting microscope (M400; Leica Microsystems, Buffalo Grove, IL, United States). Microscopic retro-reflective glass beads (P-RETRO 45-63 μm dia., Polytec Inc., Irvine, CA) were placed on the stapes to enhance measurement of the LDV signal[34]. The magnitude of the LDV

signal was adjusted using a cosine correction (1/cos(θ)) based on an estimate of the difference in angle between the primary axis of the stapes and the orientation of the LDV laser (~45°).

Baseline measurements of stapes velocity (V_{Stap}) and intracochlear pressures (P_{IC}) were made to acoustic stimuli. Input from the microphone, LDV, and pressure sensors were simultaneously captured via the sound card analog inputs. Signals acquired were band-pass filtered between 15-15000 Hz with a second order Butterworth filter.

Cochlear Implant Electrode Insertion:

After baseline responses to acoustic stimuli were recorded, a round window cochleostomy for electrode insertion was made with a fine pick. Each of three electrodes was inserted fully under water at one of three speeds (0.2 mm/s, 1.2 mm/s, or 2.0 mm/s) either by hand in accordance with manufacturer guidelines or with the use of a micro-mechanical control device (iotaMotion, Inc, Iowa City, IA). The electrodes were coupled to the insertion control device and fed through the insertion guide sheath (Figure 1B) until the electrode tip was at distal end. The device was secured at edge of mastoid cavity with bone screws (Figure 1C). A slit was then made in round window membrane and the guide sheath tip was secured at the RW niche. The corresponding CI electrode was inserted at the prescribed distance and rate. Electrode insertions were performed by resident physicians and Neurotology faculty. CI electrodes were inserted in random order, and the following were used in these experiments: Nucleus CI422 Slim Straight inserted to 20 mm (CI422; Cochlear Ltd, Sydney, Australia), FLEX 24 inserted to 24 mm (F24; Med-El, Innsbruck, Austria), and Digisonic SP EVO inserted to 24 mm (EVO; Oticon Medical, Vallauris, France).

Data Analysis:

Baseline temporal bone measurements are shown as acoustic transfer functions, which are generated by measuring the response (intracochlear pressures) of a system (the external, middle, and inner ears) to a known stimulus (acoustic energy). The resulting transfer functions are used to generate a filter and calculate an estimate of the intensity in decibels sound pressure level (dB SPL) of acoustic stimulus in the external ear canal (EAC) that would be required to generate a given pressure measurement[15]. Raw unfiltered pressure measurements are presented for each scala, and the estimated equivalent sound pressure levels (dB SPL Eq) are provided in dB SPL Peak ($20 * \log_{10}$(peak pressure / 20μPa). Differential pressure (P_{Diff}), which is thought to be the input to the cochlear partition and the driving force for auditory transduction[35–39], is calculated as the difference in pressures between scala vestibuli and scala tympani for both unfiltered pressure and estimated equivalent ear canal sound pressure. Responses were only analyzed for recordings with a signal to noise ratio greater than 6 dB, and SNR was higher than 10 dB for the majority of the recordings.

Intracochlear pressure changes with CI electrode insertion were characterized according to maximum pressure levels recorded during each insertion. Absolute peak pressures were found in each recording using the *findpeaks* function in Matlab (R2014b; The Mathworks, Inc., Natick, MA, U.S.A.). Filter criteria required peaks to a minimum peak amplitude of the

greater of either four times the standard deviation within each recording or 100 Pa, and not all insertions contained pressure levels above this threshold. In addition, pressure peaks were only assessed if they occurred within 10 ms of one another across recording locations to avoid inclusion of artifacts.

Results:

Acoustic closed-field transfer functions:

Baseline responses of V_{Stap} and P_{IC} were assessed after placement of intracochlear pressure probes and prior to making the RW cochleostomy, which provided an additional manner in which to verify the condition of each temporal bone. Mean (±SEM) closed-field acoustic transfer function magnitudes for specimens are shown in Figure 2. Responses are overlain onto the 95% confidence interval for stapes velocities[34], and the mean and the range of responses observed for intracochlear pressures reported previously by Nakajima et al[36]. Responses collected were consistent with previous reports[14,15,29,30,33].

Peak Intracochlear Pressures with Device Insertion:

Figure 3 shows a summary of the absolute maximum peak pressures observed in all recordings in all specimens for all electrodes tested by the use of the insertion tool. Figure 3A shows the unfiltered recorded raw pressures while the maximum peak pressures in estimated EAC SPL are illustrated in Figure 3B. Estimated EAC pressures recorded during electrode insertion were as high as 170 dB SPL Peak; these levels are consistent with data previously observed in our lab[15] and comparable in magnitude to high intensity acoustic stimuli. A breakdown of the absolute maximum peak pressures by insertion speed both with and without the use of insertion tool is shown in Figure 4. Figure 4A shows the unfiltered recorded raw pressures while the maximum peak pressures in estimated EAC SPL are illustrated in Figure 4B. Figure 5 shows the raw intracochlear pressure (A) and the estimated canal pressures (B) for the same data broken down by specific electrode type that was used.

Results of an n-way ANOVA, with raw peak pressures serving as the dependent variable and insertion rate, recording location, electrode type, and use of insertion device as the independent variables, revealed a significant effect of the use of the insertion tool ($F=24.66$, $p<0.0001$), but no other individual variables. A second n-way ANOVA with estimated EAC SPL serving as the dependent variable with the same independent variables demonstrated a significant effect of recording location ($F=7.81$, $p<0.0001$), but no other individual variables. Post hoc Tukey honest significant difference (hsd) pairwise comparisons for estimated equivalent EAC pressures showed significantly higher pressure in scala tympani than scala vestibuli (Table 1).

Proportion of Insertions Containing Significant Insertion Events:

Not all insertions result in a pressure spike measurable above the thresholds outlined in the methods section. The percentage of insertions with measurable events is shown in Figure 6, with data from unfiltered raw pressures recordings shown in 6A and data from calculated estimated EAC SPL illustrated in 6B. The proportion of insertions containing at least one significant event was compared between hand insertions and use of the device. Chi-Square

analysis revealed statistically significantly fewer insertions containing pressure spikes above the noise floor when the insertion tool was used for both raw unfiltered pressure (χ^2= 65.2, p<0.0001) and estimated equivalent ear canal pressure (χ^2=262, p<0.0001).

Discussion:

Consistent with our hypothesis, results presented here demonstrated a reduced magnitude and frequency of transient peaks in intracochlear pressure with robotically-controlled CI electrode insertion when compared with insertion by hand. Though several groups have described the effects of automated implantation on insertion forces[21–25,28,40–43], to the best of our knowledge, no previous report of intracochlear pressure changes with automated or robotic insertion tools exist. With the overall goal of reducing electrode insertion-related cochlear trauma, insertion force provides an *indirect* estimate of cochlear input energy and is at greater risk to be confounded by shear from internal device friction or other sources. Intracochlear pressure is a *direct* manner of characterizing cochlear input energy and may more accurately provide a method for quantifying insertion trauma.

Pressure Changes During Cochlear Implantation and Postoperative Hearing Change:

While the underlying pathophysiology of traumatic electrode insertions has not been fully determined, evidence suggests that direct damage to the basilar membrane or lateral wall results in cellular apoptosis and post-operative inflammatory cascade eventually resulting intracochlear fibrosis[44,45]. These mechanisms are thought to be the result of direct damage and material contact between the electrode and the intracochlear structures; however, the cochlea approximates a closed fluid-filled system with an opening formed in the round window membrane during cochlear implantation. During electrode placement, the intracochlear volume is temporarily increased by the volume of the electrode being inserted, thereby causing the pressure to spike in the “closed” system. The pressure is then able to return to baseline once the intracochlear fluid can escape from the opening around the electrode or through cochlear aqueduct. By decreasing both the overall rate and the variability of electrode insertion through use of a micromechanical tool, fluid may be allowed to displace out of the cochlea rather than displacing the intrascalar structures if rapid pressure events occur. Through a slow and controlled insertion, the intracochlear pressure may equilibrate and remain low on the intracochlear structure throughout the insertion. This is supported by the pressure spike differences between manual (variable velocity insertion) vs. robotically-assisted (steady velocity insertion) insertions as shown in Figure 3.

The consistency of insertion speed and the resulting pressure change may be an additional and key contributor to intracochlear damage, similar to prior studies showing insertion speed correlates with reduced insertion forces and trauma[46,47]. While a slow and steady insertion technique is ideal, the current standard of practice relies on manual forceps or a dedicated implant specific manual tool with limited ability to consistently control the insertion speed or avoid excessive forces. The clinical utility and efficacy of both aspects are dependent on the limits of human capability, as both rely on manual performance by hand. Studies show the slowest a human can insert an electrode at steady rate is 867 um/sec and humans are not capable of continuous motion slower than 250 um/sec motion rate[48]. Therefore, the results

suggest that controlling insertion variability through a micromechanical insertion control system provides more consistent insertion which may reduce intracochlear trauma and enhance preservation of residual hearing both immediately and over time.

Micro-Mechanical Control of Electrode Insertions:

Robotic control of electrode insertion has gained increasing interest as the importance of limiting trauma during implantation has become more apparent, and several papers have demonstrated the feasibility of micro-mechanical control devices in synthetic cochlear models and cadaveric specimen[21–28,40–43]. Results presented in this study were obtained with an automated, micro-mechanical insertion device that has demonstrated significantly reduced insertion forces both in a synthetic cochlear model[20] and cadaveric specimen[19]. The system tested here is compatible with multiple commercially available electrodes and enables controlled insertion rates ranging from 50 to 2000 μm/second with an accuracy of ±3 μm. The electrode insertion trajectory into the cochlea is guided through the flexible and biocompatible implanted sheath positioned at the RW niche. Through the control interface, the surgeon sets the desired insertion rate and distance parameters while continuously controlling and monitoring the insertion under direct microscopic visualization of the electrode entering the cochlea.

Other CI robotic devices discussed in the literature include a steerable, active-bending, robotically-controlled electrode array that was initially proposed by Simaan in 2006[43], with subsequent modifications to include optimal insertion path planning[42] and force-sensing capability[25]. When tested with custom designed and fabricated electrodes, the Simaan robotic system demonstrated a reduction of insertion forces up to 59.6%[25]. The extent to which these findings translate to force reduction using standard manufactured pre-bent electrodes remains to be determined.

Another prototype mechatronic device designed for an automated insertion of styleted implants was described in by Labadie in 2008[27], with the specific target of implementing the advance off-stylet (AOS) technique with the Nucleus 24 Contour Advance electrode by the Cochlear Corporation. When coupled to a force transducer in cochlear models, the device demonstrated less variability and lower peak insertion forces when compared with experienced surgeons, though the average insertion force across depth was significantly lower for surgeons[24,28,41]. Subsequent improvements in the Labadie tool include radiographic verification of insertion depth[26], integration of force-sensing capabilities[22,23], and a smaller, lighter interface[22,23]. Another additional new design for insertion of perimodiolar electrodes in a 3-degree-of-freedom parallel robot was recently presented with consistently low insertion forces, though additional study and miniaturization is still needed[21]. Taken together these studies using various mechanically controlled electrode insertion devices are generally consistent with our findings that a micro-mechanical control device significantly reduces both the overall amplitude and frequency of spikes in intracochlear pressures compared to manual electrode insertion.

Limitations:

Although this investigation represents the first description of intracochlear pressure measurements made during electrode insertion with the use of an automated insertion tool, several factors in our methodology limit the ability to generalize results from this study. Cadaveric specimen may undergo degradation and may fail to accurately depict the intracochlear environment of living patients, but they represent a more complete model than isolated temporal bones or synthetic cochlear models. Expanding methods to a similar study design with in-vivo animal testing may more closely approximate conditions in human surgery and would allow for electrophysiologic evaluation of changes in hearing. Additionally, though we have reliably characterized high-level transient pressure changes during electrode insertion in several studies, the significance of these events remains unknown. We infer the potential for cochlear damage based on the magnitude of the recorded pressure changes, but the exact mechanism for creation of these events and their impact on hearing function remains unknown.

Conclusions:

As our discipline gains greater insight into the benefits of preserved residual hearing and the potential cochlear damage associated with implantation, we have more closely examined the manner in which the surgery is performed. While “soft”, less traumatic electrode insertion techniques and array designs are commonly used to reduce the trauma associated with surgery, manual insertion is known to cause damage to the delicate intracochlear structures. Our results confirm previous data that suggest CI electrode insertion can cause pressure transients with intensities similar to those elicited by high-level sounds and affirm the importance of atraumatic surgical techniques. We suggest that use of a micro-mechanical insertion control system may help mitigate trauma from pressure events, both by reducing the amplitude and the number of pressure spikes resulting from CI electrode insertion. Continued development of automated insertion tools towards clinical use may provide one additional means for reducing cochlear trauma and maintaining residual hearing thereby improving outcomes for CI patients.

Acknowledgments

Funding: NIH 5T32DC012280-03, NIH 5T32DC000040-23 and UI OVPR&ED Gap Award.

References:

1. Roland JT, Gantz BJ, Waltzman SB, Parkinson AJ, Multicenter Clinical Trial Group. United States multicenter clinical trial of the cochlear nucleus hybrid implant system. Laryngoscope. 2016;126(1): 175–181. [PubMed: 26152811]
2. Gifford RH, Grantham DW, Sheffield SW, Davis TJ, Dwyer R, Dorman MF. Localization and interaural time difference (ITD) thresholds for cochlear implant recipients with preserved acoustic hearing in the implanted ear. Hear Res. 2014;312:28–37. [PubMed: 24607490]
3. Brown RF, Hullar TE, Cadieux JH, Chole RA. Residual hearing preservation after pediatric cochlear implantation. Otol Neurotol. 2010;31(8):1221–1226. [PubMed: 20818293]
4. Dorman MF, Gifford RH, Spahr AJ, McKarns SA. The benefits of combining acoustic and electric stimulation for the recognition of speech, voice and melodies. Audiol Neurootol. 2008;13(2):105–112. [PubMed: 18057874]

5. Turner CW, Gantz BJ, Vidal C, Behrens A, Henry BA. Speech recognition in noise for cochlear implant listeners: benefits of residual acoustic hearing. J Acoust Soc Am. 2004;115(4):1729–1735. [PubMed: 15101651]
6. Gantz BJ, Turner CW. Combining acoustic and electrical hearing. Laryngoscope. 2003;113(10): 1726–1730. [PubMed: 14520097]
7. Khater A, El-Anwar MW. Methods of Hearing Preservation during Cochlear Implantation. Int Arch Otorhinolaryngol. 2017;21(3):297–301. [PubMed: 28680501]
8. Lenarz T, Stover T, Buechner A, et al. Temporal bone results and hearing preservation with a new straight electrode. Audiol Neurotol. 2006;11 Suppl 1(1):34–41.
9. Stuermer KJ, Schwarz D, Anagiotos A, Lang-Roth R, Hüttenbrink K- B, Lüers J- C. Cochlear implantation using the underwater technique: long-term results. Eur Arch Otorhinolaryngol. 2018;275(4):875–881. [PubMed: 29417275]
10. Todt I, Mittmann P, Ernst A. Hearing Preservation With a Midscalar Electrode Comparison of a Regular and Steroid/Pressure Optimized Surgical Approach in Patients With Residual Hearing. Otol Neurotol. 2016;37(9):e349–e352. [PubMed: 27631658]
11. Nguyen S, Cloutier F, Philippon D, Côté M, Bussières R, Backous DD. Outcomes review of modern hearing preservation technique in cochlear implant. Auris Nasus Larynx. 2016;43(5):485–488. [PubMed: 26976547]
12. Miranda PC, Sampaio ALL, Lopes RAF, Ramos Venosa A, de Oliveira CACP. Hearing preservation in cochlear implant surgery. Int J Otolaryngol. 2014;2014:468515. [PubMed: 25276136]
13. Carlson ML, Driscoll CLW, Gifford RH, et al. Implications of minimizing trauma during conventional cochlear implantation. Otol Neurotol. 2011;32(6):962–968. doi:10.1097/MAO.0b013e3182204526. [PubMed: 21659922]
14. Banakis Hartl RM, Greene NT, Jenkins HA, Cass SP, Tollin DJ. Lateral Semicircular Canal Pressures During Cochlear Implant Electrode Insertion: a Possible Mechanism for Postoperative Vestibular Loss. Otol Neurotol. 2018;39(6):755–764. [PubMed: 29889786]
15. Greene NT, Mattingly JK, Banakis Hartl RM, Tollin DJ, Cass SP. Intracochlear Pressure Transients During Cochlear Implant Electrode Insertion. Otol Neurotol. 2016;37(10):1541–1548. [PubMed: 27753703]
16. Todt I, Mittmann P, Ernst A. Intracochlear fluid pressure changes related to the insertional speed of a CI electrode. Biomed Res Int. 2014;2014:507241. [PubMed: 25140316]
17. Mittmann M, Ernst A, Mittmann P, Todt I. Insertional depth-dependent intracochlear pressure changes in a model of cochlear implantation. Acta Otolaryngol. 2017;137(2):113–118. [PubMed: 27575779]
18. Mittmann P, Mittmann M, Ernst A, Todt I. Intracochlear Pressure Changes due to 2 Electrode Types: An Artificial Model Experiment. Otolaryngol Head Neck Surg. 2017;156(4):712–716. [PubMed: 28025904]
19. Henslee A, Kaufmann CR, Hansen MR. Evaluation of an Implantable Robotic-Assisted System for Cochlear Implant Insertion Control Presented at The Association for Research in Otolaryngology Midwinter Meeting; February 9, 2018; San Diego, CA.
20. Kaufmann CR, Hansen MR. Micro-mechanical Control of Cochlear Implant Electrode Insertion Decreases Maximum Insertion Forces Presented at The Association for Research in Otolaryngology Midwinter Meeting; February 11, 2017; Baltimore, MD.
21. Pile J, Simaan N. Modeling, Design, and Evaluation of a Parallel Robot for Cochlear Implant Surgery. IEEE ASME Trans Mechatron. 2014;19(6):1746–1755.
22. Kobler J- P, Beckmann D, Rau TS, Majdani O, Ortmaier T. An automated insertion tool for cochlear implants with integrated force sensing capability. Int J CARS. 2014;9(3):481–494.
23. Schurzig D, Labadie RF, Hussong A, Rau TS, Webster RJ. Design of a Tool Integrating Force Sensing With Automated Insertion in Cochlear Implantation. IEEE ASME Trans Mechatron. 2012;17(2):381–389. [PubMed: 23482414]
24. Schurzig D, Webster RJ, Dietrich MS, Labadie RF. Force of cochlear implant electrode insertion performed by a robotic insertion tool: comparison of traditional versus Advance Off-Stylet techniques. Otol Neurotol. 2010;31(8):1207–1210. [PubMed: 20814345]

25. Zhang J, Wei W, Ding J, Roland JT, Manolidis S, Simaan N. Inroads toward robot-assisted cochlear implant surgery using steerable electrode arrays. Otol Neurotol. 2010;31(8):1199–1206. [PubMed: 20864880]
26. Hussong A, Rau TS, Ortmaier T, Heimann B, Lenarz T, Majdani O. An automated insertion tool for cochlear implants: another step towards atraumatic cochlear implant surgery. Int J CARS. 2010;5(2):163–171.
27. Hussong A, Rau T, Eilers H, et al. Conception and design of an automated insertion tool for cochlear implants. Conf Proc IEEE Eng Med Biol Soc. 2008;2008:5593–5596. [PubMed: 19163985]
28. Majdani O, Schurzig D, Hussong A, et al. Force measurement of insertion of cochlear implant electrode arrays in vitro: comparison of surgeon to automated insertion tool. Acta Otolaryngol. 2010;130(1):31–36. [PubMed: 19484593]
29. Farrell NF, Banakis Hartl RM, Benichoux V, Brown AD, Cass SP, Tollin DJ. Intracochlear Measurements of Interaural Time and Level Differences Conveyed by Bilateral Bone Conduction Systems. Otol Neurotol. 2017;38(10):1476–1483. [PubMed: 29084088]
30. Banakis Hartl RM, Mattingly JK, Greene NT, Farrell NF, Gubbels SP, Tollin DJ. Drill-induced Cochlear Injury During Otologic Surgery: Intracochlear Pressure Evidence of Acoustic Trauma. Otol Neurotol. 2017;38(7):938–947. [PubMed: 28598950]
31. Maxwell AK, Banakis Hartl RM, Greene NT, et al. Semicircular Canal Pressure Changes During High-intensity Acoustic Stimulation. Otol Neurotol. 2017;38(7):1043–1051. [PubMed: 28570420]
32. Banakis Hartl RM, Mattingly JK, Greene NT, Jenkins HA, Cass SP, Tollin DJ. A Preliminary Investigation of the Air-Bone Gap: Changes in Intracochlear Sound Pressure With Air- and Bone-conducted Stimuli After Cochlear Implantation. Otol Neurotol. 2016;37(9):1291–1299. [PubMed: 27579835]
33. Mattingly JK, Greene NT, Jenkins HA, Tollin DJ, Easter JR, Cass SP. Effects of Skin Thickness on Cochlear Input Signal Using Transcutaneous Bone Conduction Implants. Otol Neurotol. 2015;36(8):1403–1411. [PubMed: 26164446]
34. Rosowski JJ, Chien W, Ravicz ME, Merchant SN. Testing a method for quantifying the output of implantable middle ear hearing devices. Audiol Neurootol. 2007;12(4):265–276. [PubMed: 17406105]
35. Ravicz ME, Rosowski JJ. Inner-ear sound pressures near the base of the cochlea in chinchilla: further investigation. J Acoust Soc Am. 2013;133(4):2208–2223. [PubMed: 23556590]
36. Nakajima HH, Dong W, Olson ES, Merchant SN, Ravicz ME, Rosowski JJ. Differential intracochlear sound pressure measurements in normal human temporal bones. J Assoc Res Otolaryngol. 2009;10(1):23–36. [PubMed: 19067078]
37. Voss SE, Rosowski JJ, Peake WT. Is the pressure difference between the oval and round windows the effective acoustic stimulus for the cochlea? J Acoust Soc Am. 1996;100(3):1602–1616. [PubMed: 8817890]
38. Lynch TJ, Nedzelnitsky V, Peake WT. Input impedance of the cochlea in cat. J Acoust Soc Am. 1982;72(1):108–130. [PubMed: 7108034]
39. Dancer A, Franke R. Intracochlear sound pressure measurements in guinea pigs. Hear Res. 1980;2(3-4):191–205. [PubMed: 7410227]
40. Miroir M, Nguyen Y, Kazmitcheff G, Ferrary E, Sterkers O, Grayeli AB. Friction force measurement during cochlear implant insertion: application to a force-controlled insertion tool design. Otol Neurotol. 2012;33(6):1092–1100. [PubMed: 22772019]
41. Rau TS, Hussong A, Leinung M, Lenarz T, Majdani O. Automated insertion of preformed cochlear implant electrodes: evaluation of curling behaviour and insertion forces on an artificial cochlear model. Int J CARS. 2010;5(2):173–181.
42. Zhang J, Roland JT Jr., Manolidis S, Simaan N. Optimal path planning for robotic insertion of steerable electrode arrays in cochlear implant surgery. J Med Devices. 2008;3(1):011001–011001–10.
43. Zhang J, Xu K, Simaan N, Manolidis S. A pilot study of robot-assisted cochlear implant surgery using steerable electrode arrays. Med Image Comput Comput Assist Interv. 2006;9(Pt 1):33–40.

44. O'Connell BP, Holder JT, Dwyer RT, et al. Intra- and Postoperative Electrocochleography May Be Predictive of Final Electrode Position and Postoperative Hearing Preservation. Front Neurosci. 2017;11:291. [PubMed: 28611574]

45. Eshraghi AA, Ahmed J, Krysiak E, et al. Clinical, surgical, and electrical factors impacting residual hearing in cochlear implant surgery. Acta Otolaryngol. 2017;137(4):384–388. [PubMed: 27918225]

46. Rajan GP, Kontorinis G, Kuthubutheen J. The effects of insertion speed on inner ear function during cochlear implantation: a comparison study. Audiol Neurootol. 2013;18(1):17–22. [PubMed: 23006502]

47. Kontorinis G, Lenarz T, Stover T, Paasche G. Impact of the insertion speed of cochlear implant electrodes on the insertion forces. Otol Neurotol. 2011;32(4):565–570. [PubMed: 21478788]

48. Kesler K, Dillon NP, Fichera L, Labadie RF. Human Kinematics of Cochlear Implant Surgery: An Investigation of Insertion Micro-Motions and Speed Limitations. *Otolaryngol Head Neck Surg*. 2017;157(3):493–498.

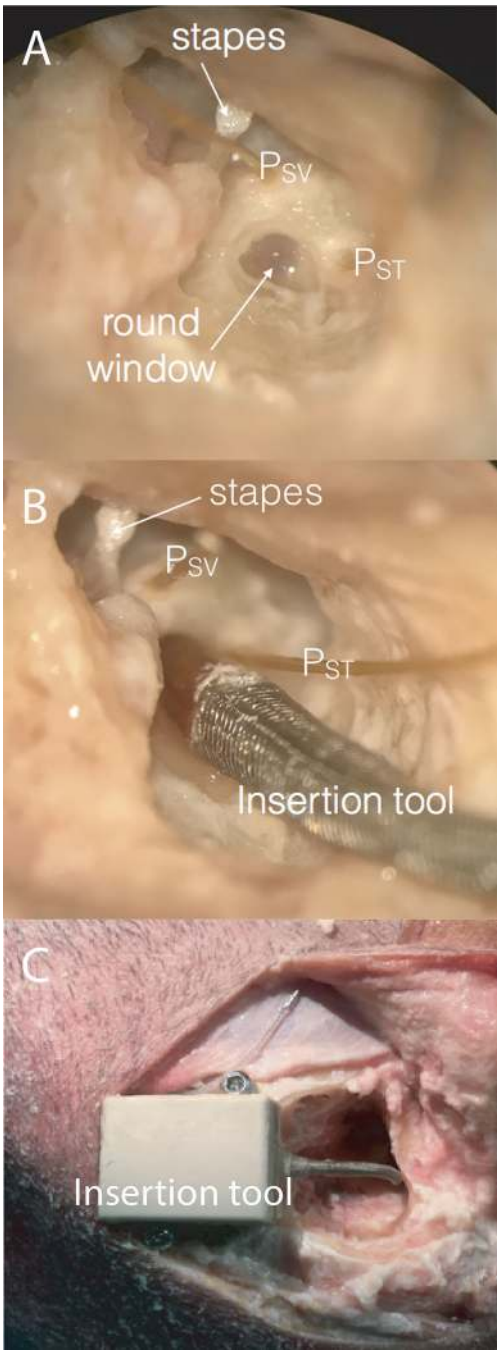

Figure 1:
Photomicrograph of the right ear in a single specimen during data collection. Through the extended facial recess, the anatomical landmarks (stapes and round window niche) can be visualized. Pressure probes (P_{SV} and P_{ST}) were placed in cochleostomies in scala vestibuli and tympani (A). The insertion tool guide sheath was placed into the round window niche to direct implant electrode placement (B). The insertion tool unit secured by bone screws at edge of mastoid cavity with electrode coupled and housed within enclosure and guide sheath (C).

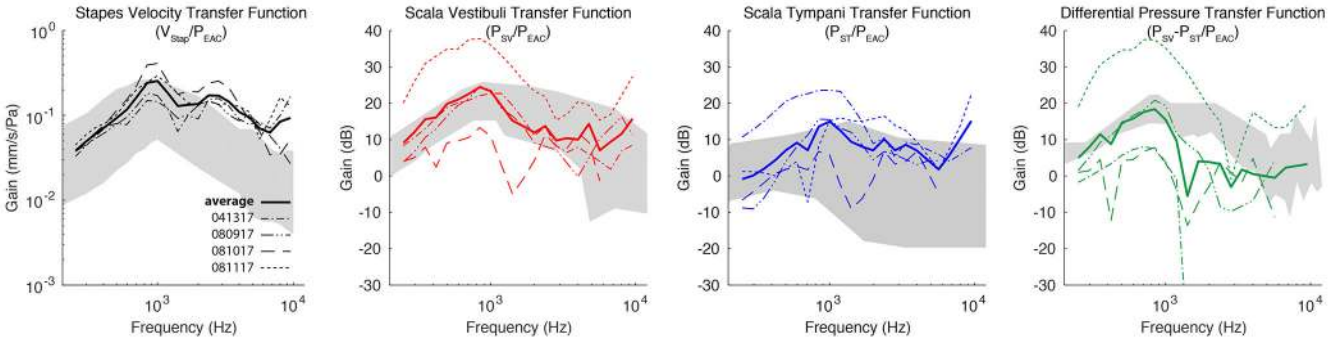

Figure 2:

Mean baseline stapes velocity (V_{Stap}), scala vestibuli pressure (P_{SV}), scala tympani pressure (P_{ST}), and differential pressure (P_{Diff}; P_{SV}-P_{ST}) transfer function magnitudes to air-conducted stimuli. Responses recorded in specimens are shown normalized to the SPL recorded in the ear canal (P_{EAC}) and are superimposed onto the 95% CI and range of responses (gray bands) observed previously[34,36]. Colored bands indicate +/− standard error of the mean.

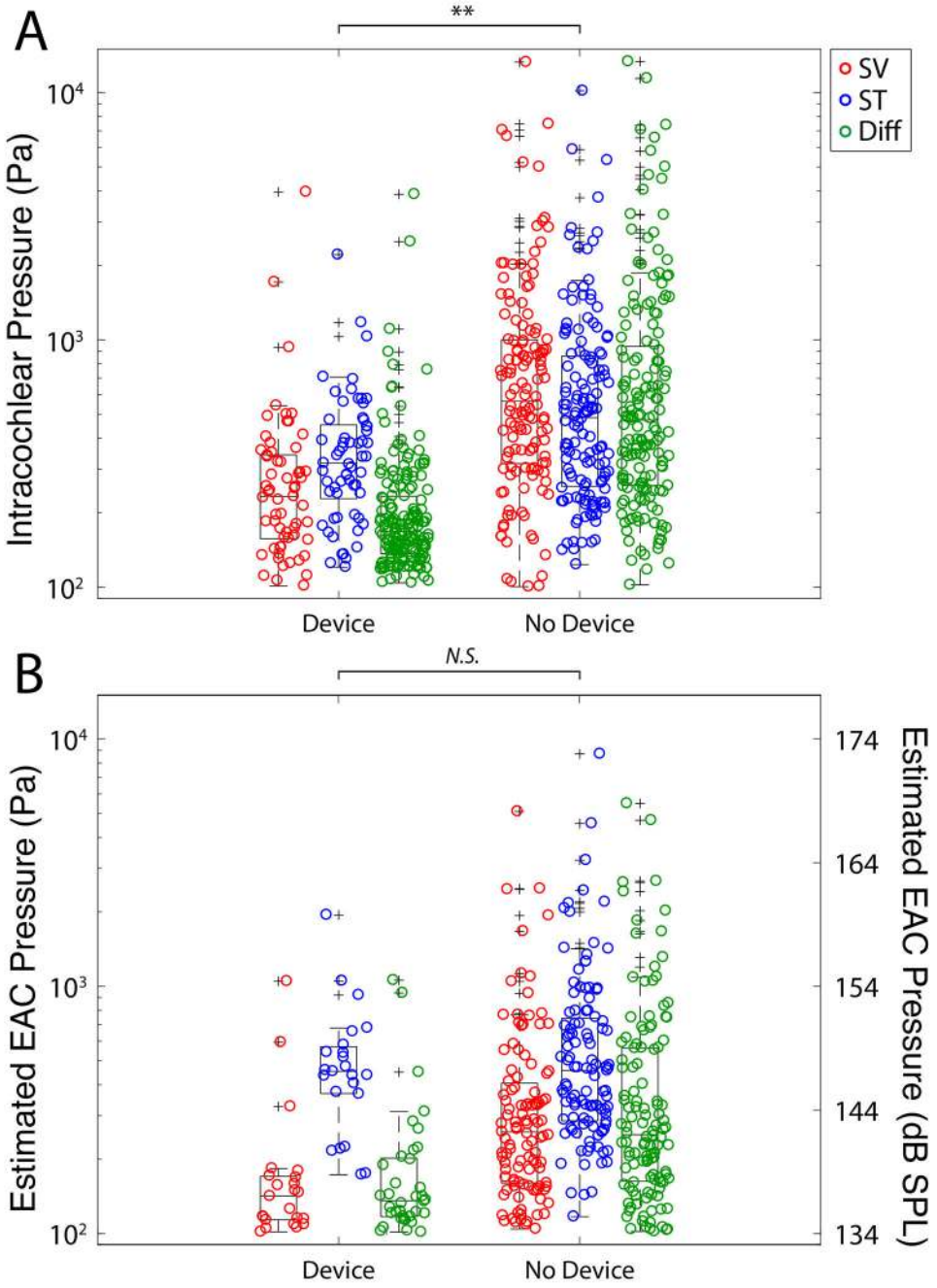

Figure 3:

Summary of peak sound pressure levels observed in all specimens during all electrode insertions. Unfiltered peak intracochlear pressure measurements (A) and estimated EAC pressures (B) are shown for each pressure recording as a function of recording location. Box plots represent the median +/−25% of the range of pressures observed, whiskers show the full range of the estimated distribution, and +'s mark outliers. Significant differences between groups are indicated with asterisks (* $p<0.05$, ** $p<0.01$).

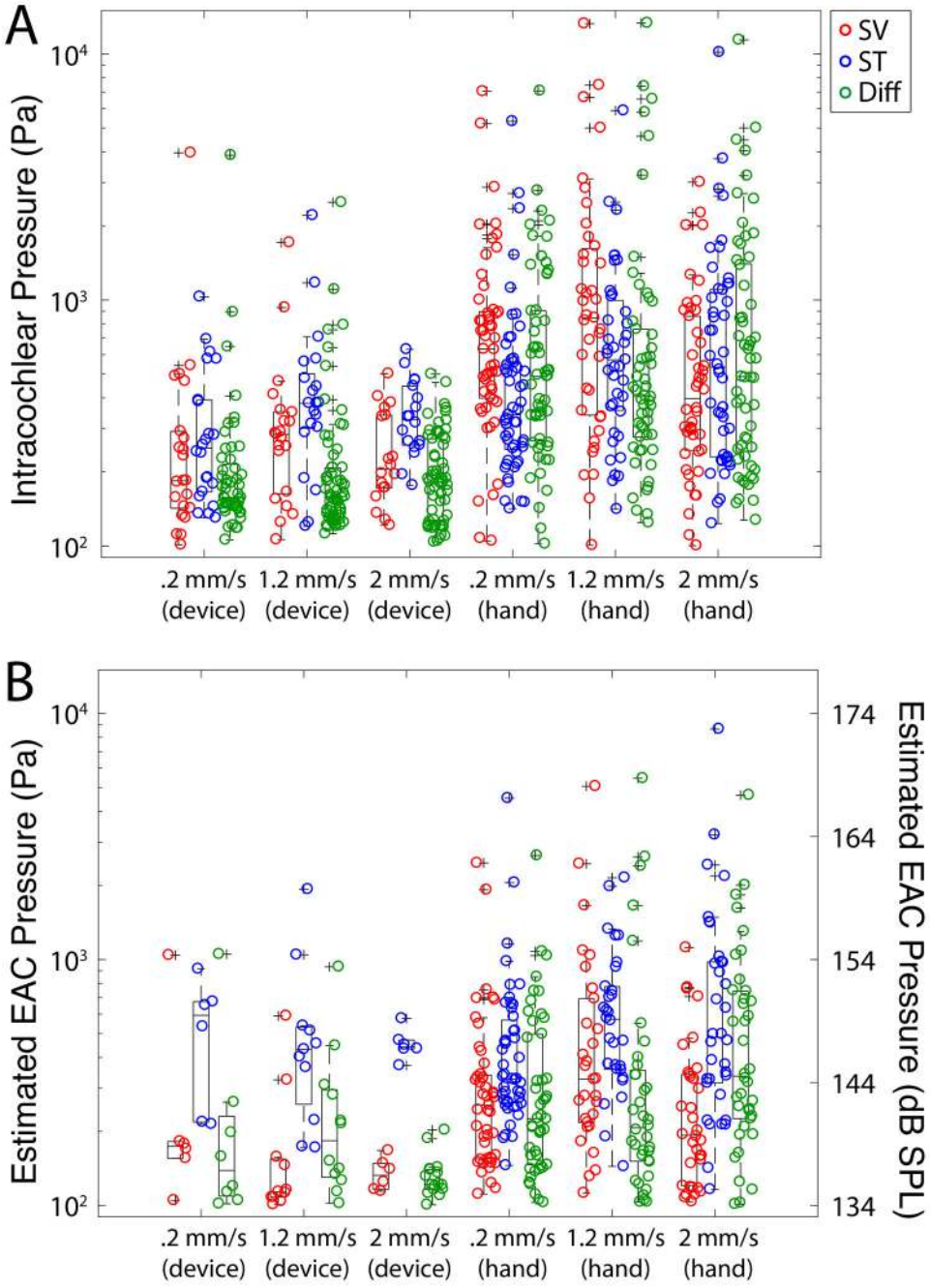

Figure 4:

Summary of peak sound pressure levels by insertion rate. Unfiltered peak intracochlear pressure measurements (A) and estimated EAC pressures (B) are shown for each pressure recording as a function of insertion speed. Box plots represent the median +/−25% of the range of pressures observed, whiskers show the full range of the estimated distribution, and +'s mark outliers. No significant differences between groups were noted.

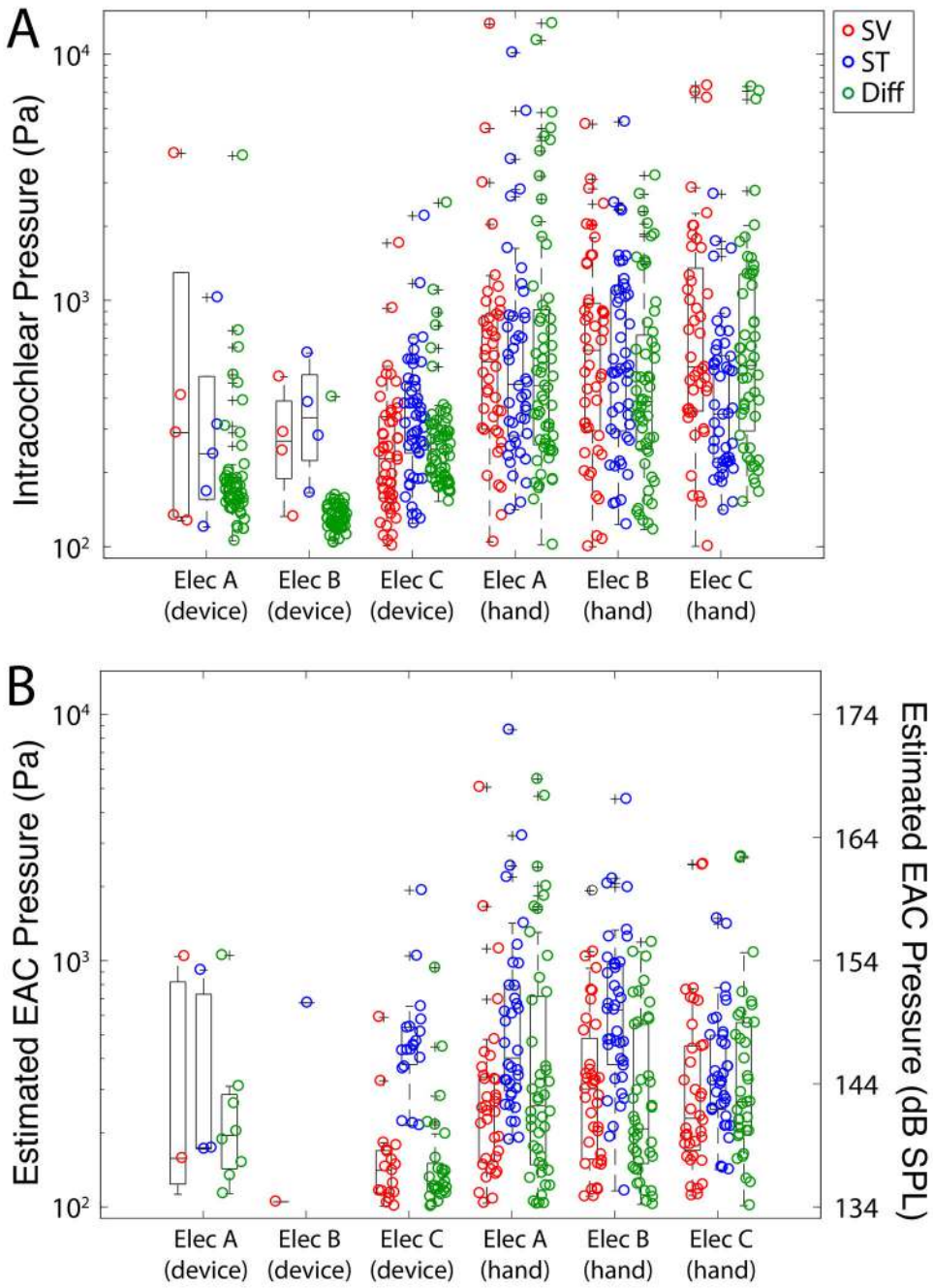

Figure 5:

Summary of peak sound pressure levels by electrode type. Unfiltered peak intracochlear pressure measurements (A) and estimated EAC pressures (B) are shown for each pressure recording as a function of electrode type. Box plots represent the median +/−25% of the range of pressures observed, whiskers show the full range of the estimated distribution, and +'s mark outliers. No significant differences between groups were noted.

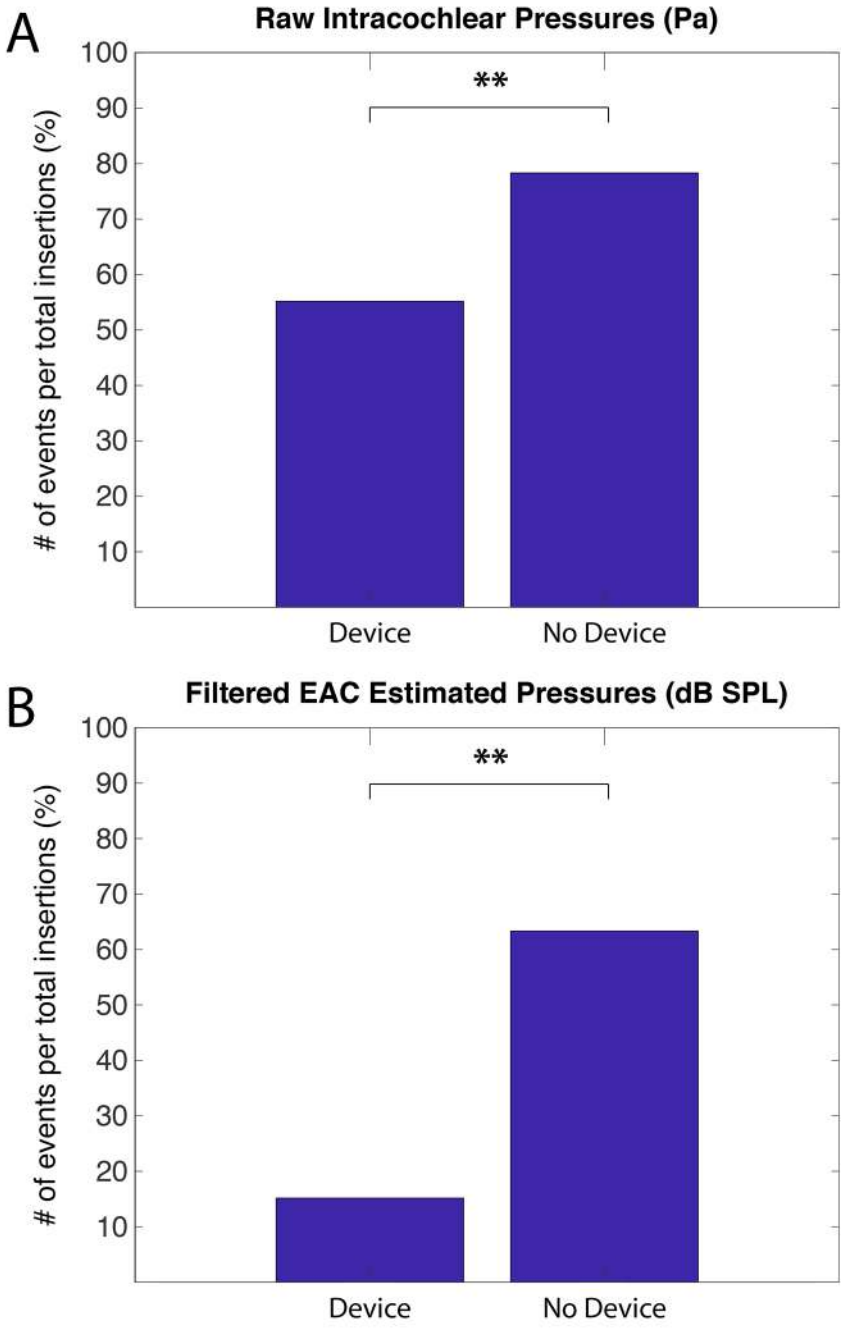

Figure 6:

Percent of insertions with a significant pressure event by insertion duration. Chi-squared analysis with Bonferroni correction revealed a significant pattern of fewer exposures with the use of the micromechanical control device. Significant differences between groups are indicated with asterisks (* $p<0.05$, ** $p<0.01$).

Table 1:

Posthoc Tukey honest-significant difference (hsd) pairwaise comparisons for estimated equivalent ear canal sound pressure level (Est Eq EAC SPL) by recording location

Location	Location	Lower limit 95% CI for true mean difference	Difference between estimated group means	Upper limit 95% CI for true mean difference	*p*-value
Diff	ST	−678.1	−399.6	−121.0	**0.002***
Diff	SV	−231.0	47.6	326.1	0.915
ST	SV	151.6	447.2	742.7	**1.14E-03***